Acta Technica *61*, No. 4B/2016, 75–86

Experimental and numerical analysis of I type crack blunt propagation mechanism[1]

S. L. Wang[2], W. Song[2], K. X. Dong[2], Y. B. Su[2], D. S. Zhang[3], C. H. Li[3]

Abstract. A complex fracture network is investigated that may occur as a consequence of crossing morphological and hydraulic fractures. The study is based on weak interface bedding and natural fractures widely-distributed in unconventional reservoirs. By constructing three-point bending test of I-type crack extension, using digital speckle correlation experiments and numerical simulation method, change laws of surface strain field, stress field, crack tip opening displacement and stress intensity factor can be obtained. Through experimental and simulation results, we know that: When I-type crack intersects with weak bedding, the crack became blunt, interfacial shear strain increases rapidly, direction of crack tip maximum circumferential stress deflects, mode I crack transforms to a mixed mode I-II crack and ratio of K_{II}/K_I increases, then the crack extends deflected.

Key words. I-type crack, blunt, shear, deflect, weak bedding.

1. Introduction

Weak bedding development of unconventional reservoirs, hydraulic fracture intersects with weak bedding and extend along it, are the keys of forming fracture network [1]. Study of the fracture morphology after artificial fracture and weak bedding intersection has important significance for understanding fracture deflected propagation mechanism and revealing the fracture network formation mechanism.

By means of theoretical and experimental methods, many scholars have analyzed

[1]Supported jointly by National Basic Research Program of China (2015CB250900), Natural Science Foundation of China (51374074) and Northeast Petroleum University Innovation Foundation for Postgraduates (yjscx2015-024nepu).

[2]College of mechanical science and engineering, Northeast Petroleum University, Daqing, 163318, China

[3]Research Institute of Oil Production Engineering of Daqing Oilfield Company Ltd, Daqing, 163712, China

the intersections of artificial fractures and natural fractures, and put forward some extended criteria: Warpinski adopted linear friction theory to consider the shear slip failure caused by the fracture surface shear stress, and analyzed the tensile failure caused by the normal stress in the crack surface by using Mohr-Coulomb criterion, and proposed W–T criterion [2]. Rehshaw and Pollard studied the induced stress field of the hydraulic fracture tip, and proposed the evaluating criterion of the hydraulic fracture through the natural fracture (R–P criterion) [3]. Gu and Weng suggested the G–W criterion by extending the R–P criterion to non-orthogonal condition and obtained the critical curve of the hydraulic fracture through natural fracture [4]. Anderson carried out experiment research of hydraulic fracture through the bonding interface and discussed the influence of friction coefficient [5]. Zhou Jian et al. established a large size three-axial hydraulic fracturing experiment, and discussed the factors that affect the direction of the hydraulic fracture after intersection with natural fracture. The above analysis provided the weak bedding opening conditions qualitatively, it did not bring the displacement field and strain field of crack, then it could not obtain the crack deflected propagation mechanism. Using digital speckle correlation method and numerical simulation method can provide the variation of strain field and displacement field, so that the method can analyze the deflected propagation mechanism from microscopic point of view.

2. Experimental study of I-type crack propagation

As it is difficult to obtain a large number of unconventional shale cores, according to similarity criterion [7, 8] the experimental specimens were processed with gypsum and clay as similar materials. The experimental length, high and thickness of specimens are 300 mm, 150 mm and 50 mm, respectively. The specimens are divided into 3 layers, and in each layer of height 50 mm a crack of dimensions (1 mm×10 mm) was prefabricated in the middle of the specimen bottom, as shown in Fig, 1.

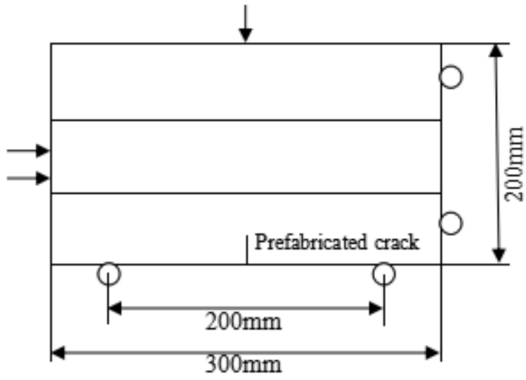

Fig. 1. Schematic diagram of material specimen

The specimens were loaded with servo loading test machine at the loading rate

of 0.03 mm/min (see Fig. 2). A high-speed video camera was used to capture the variation of the speckle field of the specimen surface. Using correlation algorithm, we can obtain the change law of displacement field and strain field in the process of the crack propagation.

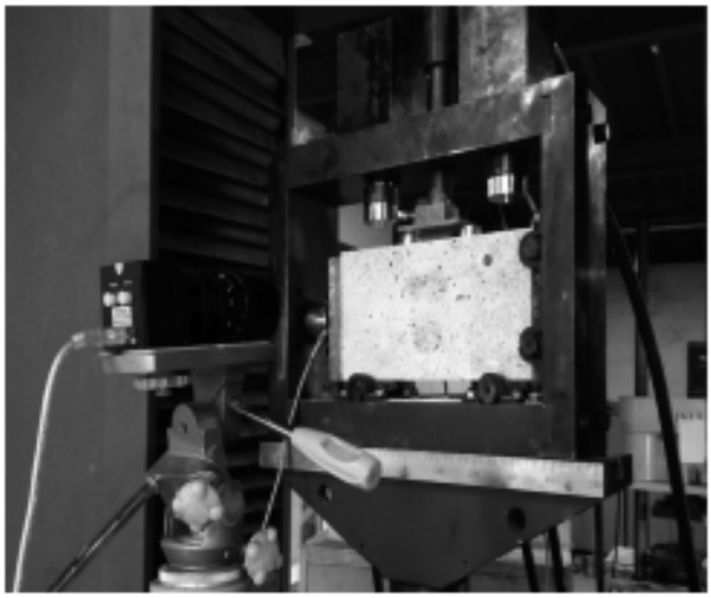

Fig. 2. Experimental loading of specimens

Figure 3 shows the evolution of horizontal strain field at different times. It can be seen from the trend of changes that with the gradual application of the load, the speckle field of the specimen surface gradually exhibits deformation localization band and extends. The final morphology of the deformation localization band is in agreement with the crack growth pattern, so that the displacement field and strain field can be used to analyze the crack propagation process.

In combination with curve in Fig. 4 we can see for loading time of 133 s that the local strain zone of the specimen surface extends to the interface position, and the relative value of the horizontal strain is 0.000116 mm at this time. For the loading time of 184 s, the local strain zone tip is still at the interface position and the length does not increase, but at this time the relative value of the horizontal strain increases rapidly to 0.001965 mm. The relative value of the horizontal strain at the crack tip is in a slow growth phase in the initial stage of loading, but from 133 s the relative value of the horizontal strain rapidly increases, and after 190 s it reaches the steady state. From this we can see that when the crack is extended to the interface, the crack tip loses the advantage of moving forward, crack growth reaches the steady state, but the crack tip opening displacement increases rapidly, and the cracks blunt phenomenon occurs here.

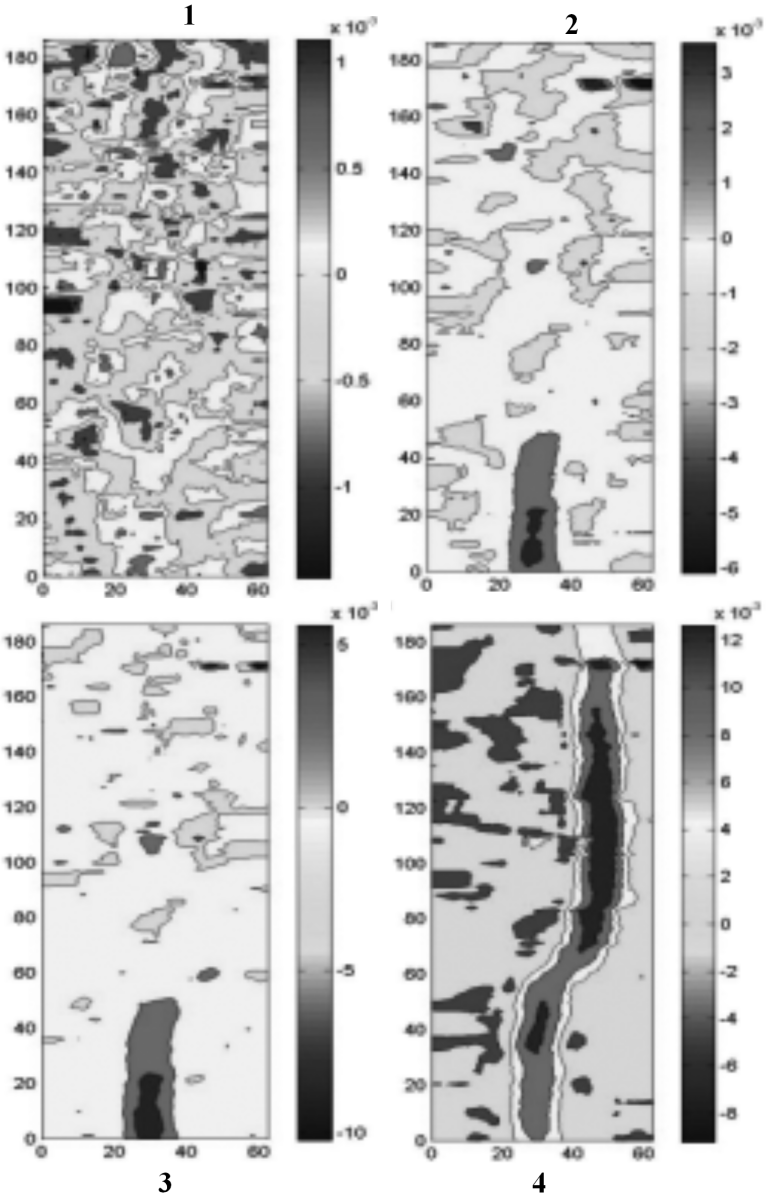

Fig. 3. Horizontal strain field changes of specimen in different times: 1–13.5 s, 2–133.6 s, 3–184 s, 4–190 s

Figure 5 shows the evolution process of shear strain field. It was shown that with the gradual application of the load, the shear strain of the crack surface also exhibits a deformation localization band. Comparison with horizontal strain field

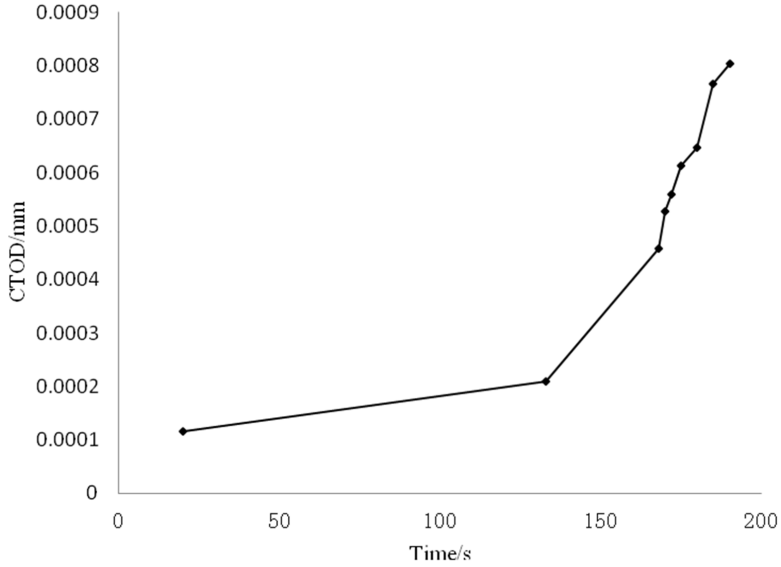

Fig. 4. Time evolution of horizontal strain field

shows that localization band appear at the interface layer. It explains that when crack extends to the interface layer where crack and interface layer join together, the interface shear concentrates there.

Figure 6 shows the distribution of shear strain in the interface layer at different times and different locations. It is obvious that shear strain of the interface increases gradually after crack extends to the interface layer. It reached the maximum 0.006848 mm after 190 s, which is much higher than in other places.

Curves in Fig. 7 show the distributions of shear strain at different horizontal positions for loading time of 190 s. The slice a was located at the interface layer, and points b, c and d were located at the upper part of the interface layer. By contrast, it is obvious that the shear strain of the interface layer is higher than the those in other horizontal positions. Upward from the interface layer, the shear strain decreases gradually and the maximum gradually decreases from 0.006848 mm to 0.005871 mm, then to 0.004126 mm and finally to 0.001644 mm. It can be seen from the above analysis that the crack gradually extends to the interface layer with the load application. After a period of time, the crack stops growing and the horizontal strain increases rapidly at the crack tip. It indicates that when the crack tip open displacement increases rapidly, it is at the blunt stage. Meanwhile, shear strain of the interface layer increases rapidly and is much higher than in other locations. Subsequently, the crack passes through the interface and extends inflected. Therefore, increase of shear strain which results in crack blunt at the interface layer, is the governing factor of inflected crack extension.

Based on the calculation method of stress intensity factor of I- and II-type crack, the crack tip opening displacement and sliding displacement are extracted, and the

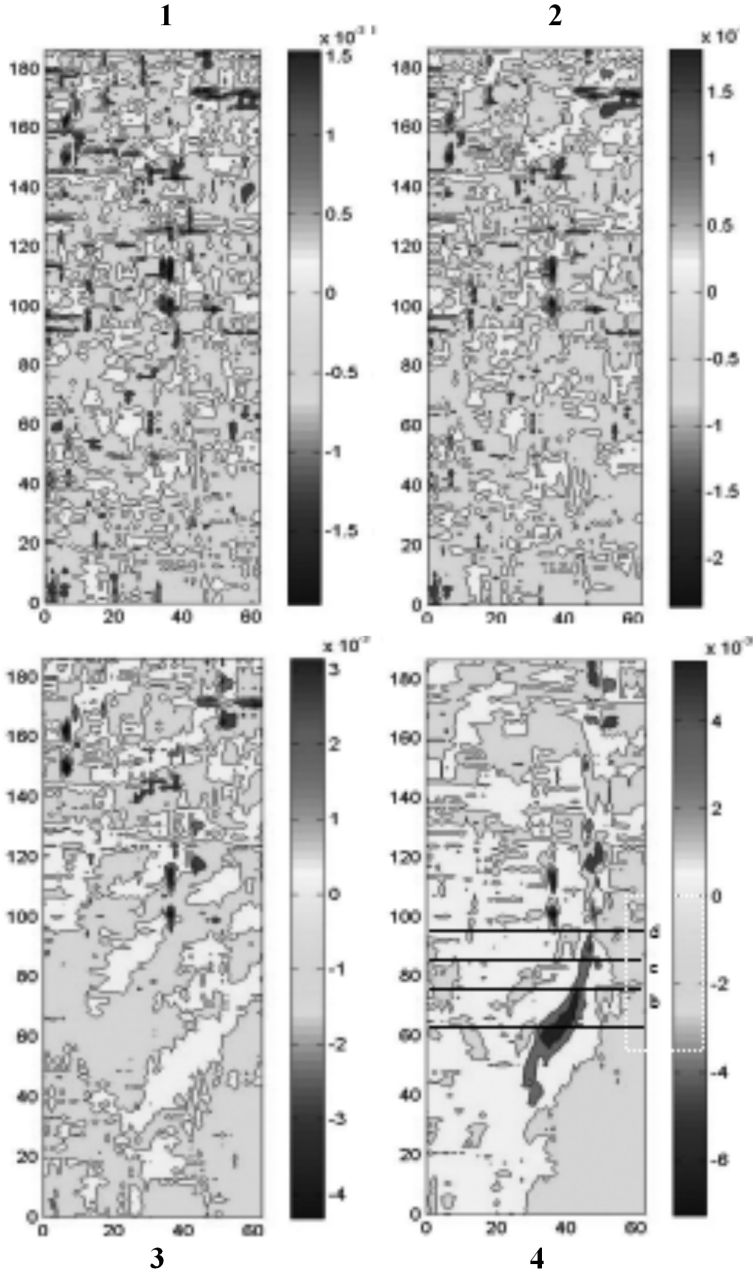

Fig. 5. Shear strain field changes of specimen in different times: 1–13.5 s, 2–133.6 s, 3–184 s, 4–190 s

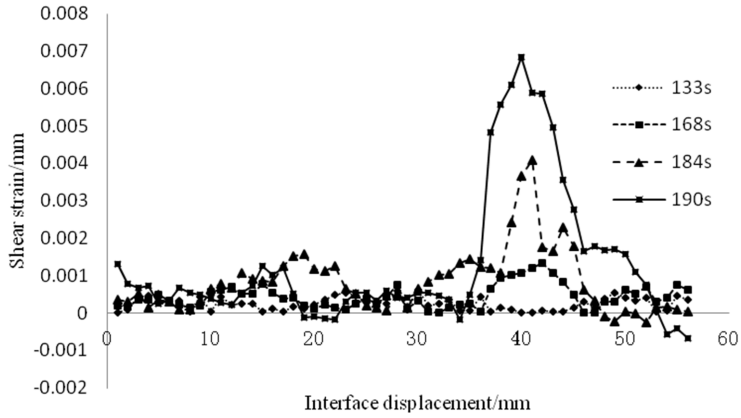

Fig. 6. Time evolution of shear strain field change curve

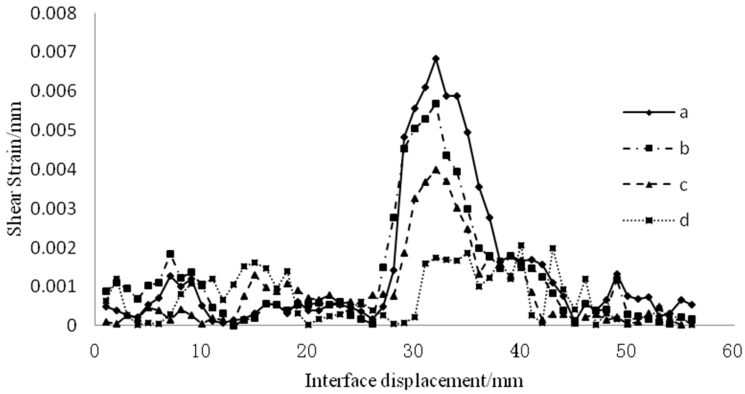

Fig. 7. Shear strain field change curve at different positions

crack tip K_I and K_{II} are calculated. At the time of 133 s, the crack tip K_I value is 0.12 MPa mm$^{0.5}$, K_{II} value is 0.0005 MPa mm$^{0.5}$. It is obvious that the K_I value is far greater than the K_{II} value, so that the latter one can be ignored. So before reaching the interface bedding, the crack is I-type open crack. With the load application, K_I gradually increases up to 5.01 MPa mm$^{0.5}$ at the time of 190 s, while the K_{II} value gradually increases to 2.04 MPa mm$^{0.5}$ and the value of K_{II}/K_I is 0.407. Coefficient K_{II} has an impact on the expansion of the crack. The crack changes from I-type to I-II composite crack, and then the crack extends deflected, the deflection angle being about 37 degrees.

3. Simulation study of I-type crack propagation

According to the three-point bending test method, the mechanical model of I-type crack propagation was established, and the geometrical size, force and boundary condition of the model are shown in Fig. 8. The finite element software ABAQUS is used to calculate the finite element model of three point bending with initial crack. The finite element model is shown in Fig. 9, where the fixed support model is applied on the left, the sliding bearing is applied on the right, while in the middle of the bottom span displacement load is applied, the speed of which being 0.03 mm/min. CPE4 elements are used for the discretization grid. In order to analyze the crack propagation, the grid encryption processing is adopted at the interface position.

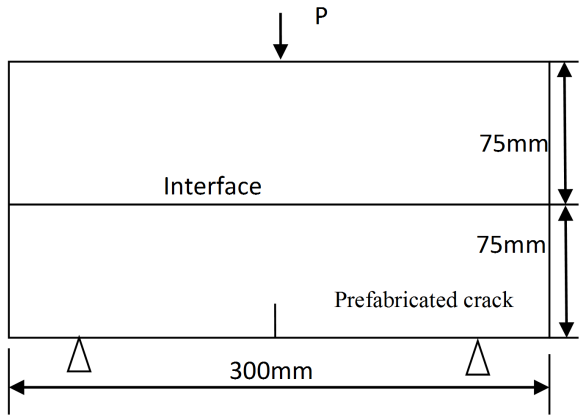

Fig. 8. Mechanical model of three-point bending

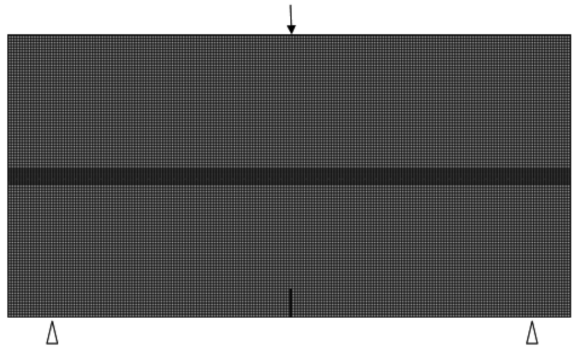

Fig. 9. Finite element model of three-point bending

Three following Figs. 10, 11 and 12 show evolutions of the crack. For better visibility, some parts are magnified.

Figure 13 shows that along with the load application, the crack length increases linearly with the load step, crack extends to the interface layer after 51 steps, crack

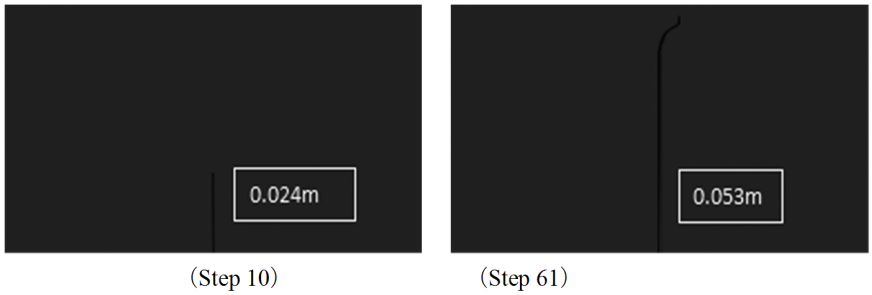

Fig. 10. Time evolution of crack propagation

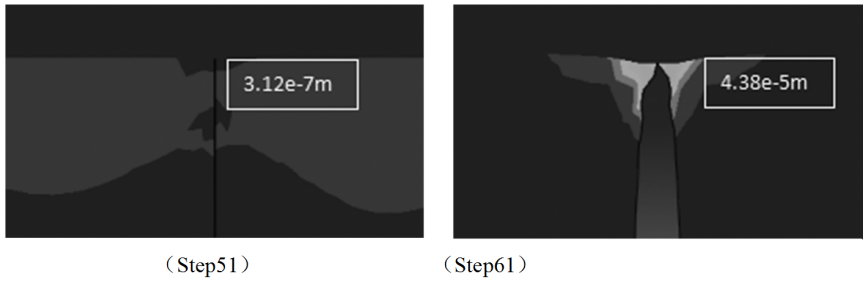

Fig. 11. Crack tip morphology in different times (magnified ten times)

Fig. 12. Time evolution of circumferential principal stress of crack tip

growth length is 46 mm, and crack length is the same after 61 steps, which says that between the 51st step to 61st step, the crack does not extend forward. From 70th step the crack continues to extend again, but the direction of propagation changes.

Figure 14 shows that after the crack extends to the interface layer, with the increase of the load step the crack tip opening displacement increases rapidly, from $3.12 \cdot 10^{-7}$ m (51st step) to $4.385 \cdot 10^{-5}$ m (61st step).

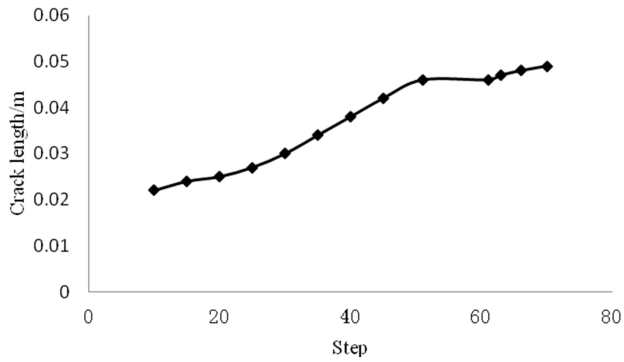

Fig. 13. Crack propagation length vs. number of steps

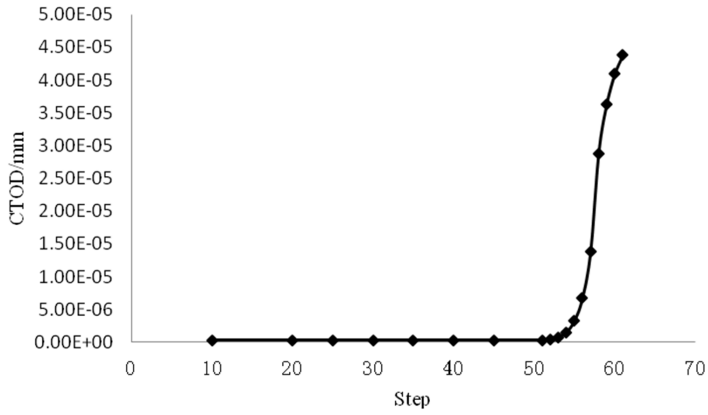

Fig. 14. Curve of crack tip opening displacement changes vs. loading step

4. Conclusion

In this paper, through the experimental and numerical simulation of I-type crack propagation, the following conclusions are obtained:

1. After I-type crack extends to the interface layer, as the interface strength is relatively low, the crack extend pauses, the crack tip opening displacement increases, and the I-crack tip decouples and blunts.

2. During the crack blunt process, the interfacial shear strain increases rapidly and interface shear strain is larger than other positions of shear strain. II-type stress intensity factor increases the crack tip to the maximum circumferential principal stress deflection, and I-type crack changes to I-II composite crack.

3. I-type crack tip caused by weak bedding, increased interfacial shear stress, maximum circumferential principal stress direction deflection, and crack tran-

sition from I-type to I-II type composite crack is are main control mechanisms of deflected crack extension.

References

[1] J. E. Olson, A. D. Taleghani: *Modeling simultaneous growth of multiple hydraulic fractures and their interaction with natural fractures.* SPE Hydraulic Fracturing Technology Conference, 19–21 Jan. 2009, The Woodlands, Texas, USA, paper SPE-119739-MS.

[2] N. R. Warpinski, L. W. Teufel: *Influence of geologic discontinuities on hydraulic fracture propagation.* J Petroleum Technology *39* (1987), No. 2, 209–220.

[3] C. E. Renshaw, D. D. Pollard: *An experimentally verified for propagation across unbounded frictional interfaces in brittle linear elastic materials.* IJ Rock Mechanics and Mining Sciences & Geomechanics Abstracts. *32* (1995), No. 3, 237–249.

[4] H. Gu, X. Weng, J. B. Lund, M. G. Mack, U. Ganguly, R. Suarez-Rivera: *Hydraulic fracture crossing natural fracture at no orthogonal angles: a criterion and its validation.* Proc. IC SPE Production and Operations, 24–26 Jan. 2012, The Woodlands, TexasUSA, 20–26.

[5] C. D. Anderson: *Effects of friction on hydraulic fracture growth near unbounded interfaces in rocks.* Society of Petroleum Engineers Journal *21* (1981), No. 1, 21–29.

[6] W. Burgert, M. Lippmann: *Models of translatory rock bursting in coal.* IJ Rock Mechanics and Mining Science & Geomechanics Abstracts *18* (1981), No. 4, 285–294.

[7] J. Marzbanrad, G. Soleimani, M. Mahmoodi-k, A. H. Rabiee: *Development of fuzzy anti roll bar controller for improving vehicle stability.* J Vibroengineering *17* (2015), No. 7, 3856–3864.

[8] H. Zhang, H. Song, Y. Kang, G, Huang, C. Qu: *Experimental analysis on deformation evolution and crack propagation of rock under cyclic indentation.* Rock Mech. Rock Eng. *46* (2013), No. 5, 1053–1059.

Received November 16, 2016